

The New Physics at RHIC. From Transparency to High p_t Suppression.

J. J. Gaardhøje⁷ for the BRAHMS Collaboration

I. Arsene¹⁰, I. G. Bearden⁷, D. Beavis¹, C. Besliu¹⁰, B. Budick⁶, H. Bøggild⁷,
C. Chasman¹, C. H. Christensen⁷, P. Christiansen⁷, J. Cibor³, R. Debbe¹, E. Enger¹²,
J. J. Gaardhøje⁷, M. Germinario⁷, K. Hagel⁸, O. Hansen⁷, A. Holm⁷, H. Ito^{1,11},
A. Jipa¹⁰, F. Jundt², J. I. Jørdre⁹, C. E. Jørgensen⁷, R. Karabowicz⁴, E. J. Kim¹,
T. Kozik⁴, T. M. Larsen¹², J. H. Lee¹, Y. K. Lee⁵, S. Lindal¹², R. Lystad⁹,
G. Løvholden¹², Z. Majka⁴, A. Makeev⁸, B. McBreen¹, M. Mikelsen¹², M. Murray^{8,11},
J. Natowitz⁸, B. Neumann¹¹, B. S. Nielsen⁷, J. Norris¹¹, D. Ouerdane⁷, R. Płaneta⁴,
F. Rami², C. Ristea¹⁰, O. Ristea¹⁰, D. Röhrich⁹, B. H. Samset¹², D. Sandberg⁷,
S. J. Sanders¹¹, R. A. Scheetz¹, P. Staszczak^{7,4}, T. S. Tsvetov¹², F. Videbæk¹, R. Wada⁸,
Z. Yin⁹, I. S. Zgura¹⁰

¹ Brookhaven National Laboratory, Upton, New York 11973, USA

² Institut de Recherches Subatomiques and Université Louis Pasteur, Strasbourg, France

³ Institute of Nuclear Physics, Krakow, Poland

⁴ M. Smoluchowski Inst. of Physics, Jagiellonian University, Krakow, Poland

⁵ Johns Hopkins University, Baltimore 21218, USA

⁶ New York University, New York 10003, USA

⁷ Niels Bohr Institute, University of Copenhagen, Copenhagen 2100, Denmark

⁸ Texas A&M University, College Station, Texas, 17843, USA

⁹ University of Bergen, Department of Physics, Bergen, Norway

¹⁰ University of Bucharest, Romania

¹¹ University of Kansas, Lawrence, Kansas 66045, USA

¹² University of Oslo, Department of Physics, Oslo, Norway

Heavy ion collisions at RHIC energies (Au+Au collisions at $\sqrt{s_{NN}} = 200$ GeV) exhibit significant new features as compared to earlier experiments at lower energies. The reaction is characterized by a high degree of transparency of the collisions partners leading to the formation of a baryon-poor central region. In this zone, particle production occurs mainly from the stretching of the color field. The initial energy density is well above the one considered necessary for the formation of the Quark Gluon Plasma, QGP. The production of charged particles of various masses is consistent with chemical and thermal equilibrium. Recently, a suppression of the high transverse momentum component of hadron spectra has been observed in central Au+Au collisions. This can be explained by the energy loss experienced by leading partons in a medium with a high density of unscreened color charges. In contrast, such high p_t jets are not suppressed in d+Au collisions suggesting that the high p_t suppression is not due to initial state effects in the ultrarelativistic colliding nuclei.

1. Introduction

With the Relativistic Heavy Ion Collider, RHIC, at Brookhaven National Laboratory a new chapter in the story of the production and study of nuclear matter at extreme energy density and temperature is being written. In collisions between gold nuclei at 100AGeV+100AGeV at RHIC the total energy in the center of mass is almost 40TeV, the largest so far achieved in nucleus-nucleus collisions under laboratory conditions. This energy is so large that if a sizeable fraction of the initial kinetic energy can be converted into matter production, many thousands of particles can be created in a limited volume. It is expected that a region of matter consisting of free quarks and gluons may be formed in the early stages of the collision, the so called Quark Gluon Plasma (QGP). The salient questions to answer are: how much of the initial (longitudinal) kinetic energy is converted to other degrees of freedom, what is the energy density achieved and are there specific signals that carry evidence for the nature of the formed high density state (i.e. is it partonic or hadronic)? In this talk I will try to answer some of these questions based on the results from the first rounds of experiments with RHIC.

RHIC started beam operations in the summer of year 2000 with a short commissioning run colliding Au nuclei at $\sqrt{s_{NN}} = 130$ GeV). The first full run at top energy ($\sqrt{s_{NN}} = 200$ GeV) took place in the fall/winter of 2001/2002. The third RHIC run during the winter/spring of 2003 focussed on d+Au and p+p reactions. Here, I concentrate on results from the BRAHMS detector, one of the four major detectors at RHIC, from the two long production runs. BRAHMS is a two arm magnetic spectrometer with excellent momentum resolution and particle identification capabilities for hadrons. The spectrometers subtend only a small solid angle (a few msr) but they can rotate in the horizontal plane about the collision point enabling the collection of data on hadron production over a wide rapidity range (0-4), a unique feature among the RHIC experiments. Details about the BRAHMS detector system may be found in [1,2].

2. Transparency at RHIC

The stopping of colliding nuclei is a long standing subject. In reactions at energies in the MeV domain atomic nuclei behave like droplets. In gentle collisions, nuclei can fuse forming an excited compound system at rest in the CM frame. In somewhat more violent collisions the droplets may splash and fragment with approximately isotropic distributions in the CM. Even at energies of several GeV pr. nucleon, f.for example in reactions with Au ions at the AGS, where the energy in the nucleon nucleon center of mass system is $\sqrt{s_{NN}} = 5$ GeV, the colliding nuclei, as seen from the CM frame, experience significant stopping and a large fraction of the initial kinetic energy is converted into excitations which subsequently decay and release energy for example in a direction transverse to the beam direction.

A useful way to quantify the stopping is by the rapidity loss experienced by the baryons in the colliding nuclei. Rapidity is defined as

$$y = \frac{1}{2} \ln \left(\frac{E + p_z}{E - p_z} \right) = \frac{1}{2} \ln \left(\frac{1 + \beta \cos \theta}{1 - \beta \cos \theta} \right) \quad (1)$$

where E , p_z , β and θ denote the total energy, longitudinal momentum, velocity and angle

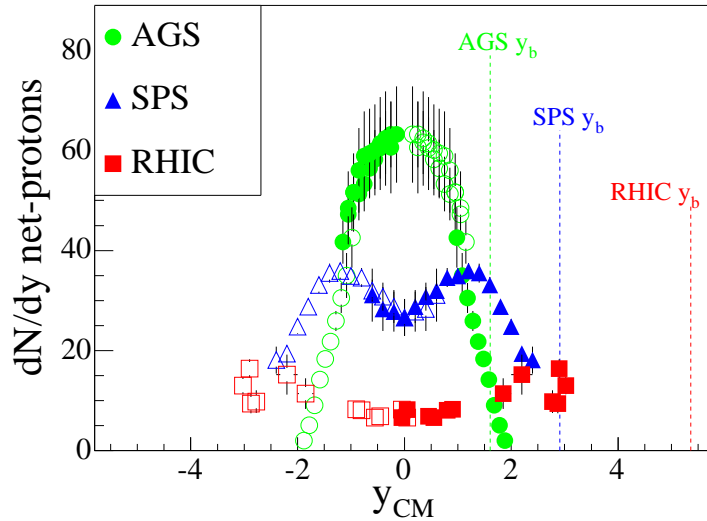


Figure 1. Preliminary rapidity densities of net protons (i.e. number of protons minus antiprotons) measured at AGS, SPS, and RHIC(BRAHMS). At RHIC, the full distribution cannot be measured with current experiments, but BRAHMS will be able to extend its measurements to $y=3.5$ in coming runs, corresponding to measurements at 2.3 degrees with respect to the beam.

relative to the beam axis, respectively, of a particle. If incoming beam baryons have rapidity, y_b relative to the CM (which has $y = 0$) and average rapidity

$$\langle y \rangle = \int_0^{y_b} y \frac{dN}{dy} dy \quad (2)$$

after the collision, the rapidity loss is $\delta y = y_b - \langle y \rangle$. Here dN/dy denotes the number of particles per unit of rapidity. Thus, for the extreme case of full stopping: $\delta y = y_b$. This corresponds to the situation found at very low energies where all the beam baryons lose all their kinetic energy. In the expression above a complication arises at CM energies large enough to allow for the formation of baryon-antibaryon pairs. Thus the baryon dN/dy distribution to be used is that for the net number of baryons (i.e. the difference between the number of baryons and antibaryons).

At AGS the number of produced antibaryons is quite small and the net-baryon distribution is similar to the proton distribution. The net-proton rapidity distribution is centered around $y = 0$ and is rather narrow. The rapidity loss is about 1 for a beam rapidity of approx. 1.6. At CERN-SPS energies ($\sqrt{s_{NN}} = 17$ GeV, 158 AGeV Pb+Pb reactions) the rapidity loss is about 2 for a beam rapidity of 2.9, about the same relative rapidity loss as at AGS. The fact that the rapidity loss is large on an absolute scale means, however, that there is still a sizeable energy loss of the colliding nuclei. This energy is available for particle production and other excitations. Indeed, in collisions at SPS, multiplicities of charged hadrons are about $dN/dy=180$ around $y=0$. At SPS another feature is visible (see fig. 1): the net proton rapidity distribution shows a double 'hump' with a dip around $y=0$. This is a consequence of two effects: the finite rapidity loss of the colliding nuclei and the finite width of each of the humps, which reflect the

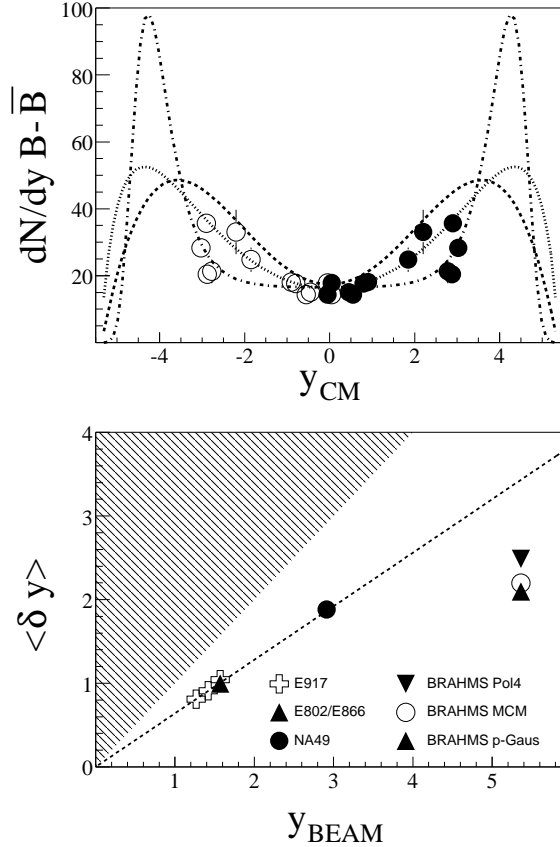


Figure 2. Upper panel: estimates of possible net-baryon distributions requiring baryon number conservation. We have assumed that $N(n) \approx N(p)$ and scaled hyperon yields at midrapidity to forward rapidity using HIJING. From these extremes, limits on the rapidity loss of colliding Au ions at RHIC can be set (lower panel). The BRAHMS data are preliminary.

rapidity distributions of the protons in the colliding nuclei after the collisions. This picture suggests that the reaction at SPS is beginning to be transparent in the sense that fewer of the original baryons are found at midrapidity after the collisions, in contrast to the situation at lower energies.

We have measured the net proton rapidity distribution at RHIC in the interval $y = 0-3$ in the first run with (0-10%) central Au+Au collisions at full energy. The beam rapidity at RHIC is about 5.4. Details of the analysis may be found in refs.[3] and in the recent Ph.D. thesis of P. Christiansen. The results are displayed in fig. 1 together with the previously discussed net-proton distributions measured at AGS and SPS. It is notable that the RHIC distribution is both qualitatively and quantitatively different from those at lower energies. The net number of protons per unit of rapidity around $y=0$ is only about 7 and the distribution is flat over at least the first unit of rapidity. The distribution increases in the rapidity range $y = 2-3$ to an average $dN/dy \approx 12$. We have not yet completed the measurements at the most forward angles (highest rapidity) allowed by the geometrical setup of the experiment, but we can exploit that there must be baryon

conservation in the reactions to try to set limits on the relative rapidity loss at RHIC. This is illustrated in fig. 2, which shows various possible distributions whose integral areas correspond to the number of baryons present in the overlap between the colliding nuclei. From such distributions one may deduce a set of upper and lower limits for the rapidity loss at RHIC. In practice the situation is complicated by the fact that not all baryons are measured. We measure in BRAHMS the direct protons, but only some of the decay protons from for example Λ . The limits shown in the figure include some reasonable estimates of these effects [3,6].

The conclusion is that the *absolute* rapidity loss at RHIC ($\delta y = 2.2 \pm 0.4$) is not appreciably larger than at SPS. In fact the *relative* rapidity loss is significantly reduced as compared to an extrapolation of the low energy systematics [4]. It should be noted that the rapidity loss is still significant and that, since the overall beam energy (rapidity) is larger at RHIC than at SPS, the absolute energy loss increases appreciably from SPS to RHIC thus making available a significantly increased amount of energy for particle creation in RHIC reactions.

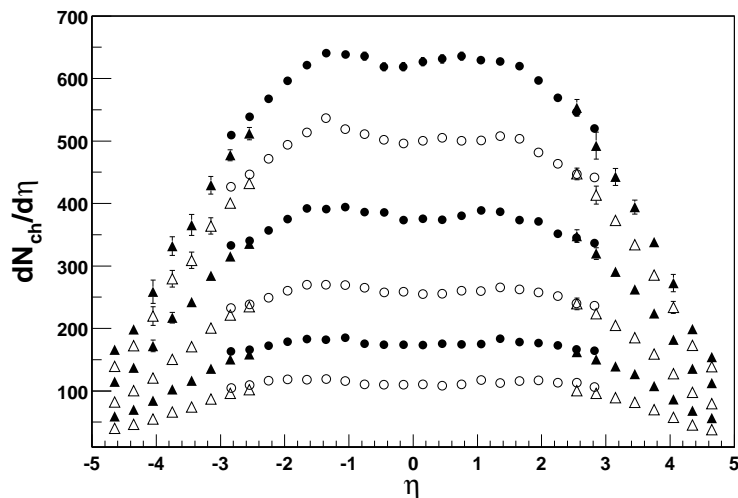


Figure 3. Pseudorapidity densities (multiplicities) of charged particles measured by BRAHMS for $\sqrt{s_{NN}} = 200$ GeV Au+Au collisions. The various distributions correspond to collisions centralities 0-5% (top), 5-10%, 10-20%, 20-30%, 30-40%, 40-50%. The integral of the most central distribution corresponds to about 4600 charged particles [2].

3. Particle production and energy density

The stopping scenario that we observe at RHIC and which was outlined in the previous section entails that the reaction can be viewed as quite transparent (opaque is perhaps a better word). After the collision, the matter and energy distribution can be conceptually divided up into two main parts, namely a so-called fragmentation region consisting of the excited remnants of the colliding nuclei which have experienced an average rapidity loss of about 2.2 and a central region in which few of the original baryons are present but where significant energy density is collected. This picture is consistent with the

schematic one already proposed by Bjorken 20 years ago [5]. The central region (an interval around midrapidity) is decoupled from the fragments. The energy removed from the kinetic energy of the fragments is initially stored in a color field strung between the receding partons that have interacted. The linear increase of the color potential with distance eventually leads to the production of quark-antiquark pairs. Such pairs may be produced anywhere between the interacting partons leading to an approximately uniform particle production as a function of rapidity. In this picture, the properties of the particle production is also uniform as a function of rapidity (boost invariance). If the density of produced quark-antiquark pairs is sufficiently high, the average distance between them will be low and the binding potential between the colored objects will be small. The objects will become asymptotically free and exist in a plasma like state until the subsequent expansion and lowered density leads to confinement and hadronization.

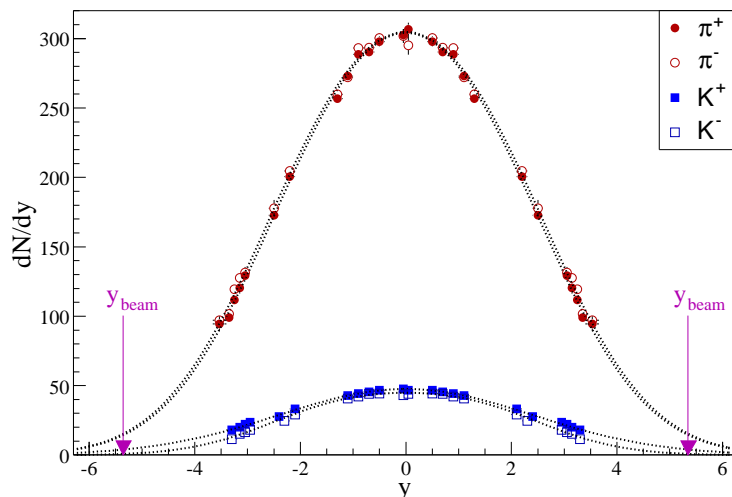


Figure 4. Rapidity density distribution for positive and negative pions and kaons. Data points collected at positive y have been reflected around $y=0$. Preliminary BRAHMS data.

Figure 3 shows the overall multiplicity of charged particles observed in Au+Au collisions at RHIC [2,7] for various collision centralities and as a function of pseudorapidity (pseudorapidity, η , is defined as $\eta = \ln(\cot(\theta/2))$ and is a customary rapidity variable for non identified particles). The figure shows that the multiplicity at RHIC is about $dN/d\eta = 625$ charged particles pr. unit rapidity around $\eta = 0$ for central collisions. The production of charged particles in central collisions exceeds the particle production seen in p+p collisions at the same energy by about 40%, when the yield seen in p+p collisions is multiplied by the number of participant nucleon pairs in the overlap region between the colliding nuclei.

Figure 4 shows a recent and more detailed study of the particle production in central collisions as a function of rapidity (the PhD. work of Djamel Ouerdane [14]). The figure shows the rapidity densities of pions and kaons for central collisions. From such distributions we can construct the ratio of the yields of particles and their antiparticles

as a function of rapidity. Figure 5 shows the ratios of yields of antihadrons to hadrons (positive pions, kaons and protons and their antiparticles). The ratio is seen to be approaching unity in an interval of about 1.5 units of rapidity around midrapidity, suggesting that the particle production is predominantly from pair creation. This is exactly true for pions (ratio of 1), but less so for kaons (ratio= 0.95) and protons (ratio= 0.76). The reason is that there are other processes that break the symmetry between particles and antiparticles that depend on the net-baryon distribution discussed in the previous section. One such process that is relevant for kaons is the associated production mechanism (e.g. $p + p \rightarrow p + \Lambda + K^+$) which leads to an enrichment of positive kaons in regions where there is an excess of baryons. Support for this view is given by fig. 6, which shows the systematics of kaon production relative to pion production as a function of center of mass energy. At AGS, where the net proton density is high at midrapidity, the rapidity density of K^+ strongly exceeds that of K^- . In contrast, at RHIC, production of K^+ and K^- is almost equal. This situation changes, however, at larger rapidities where the net proton density increases.

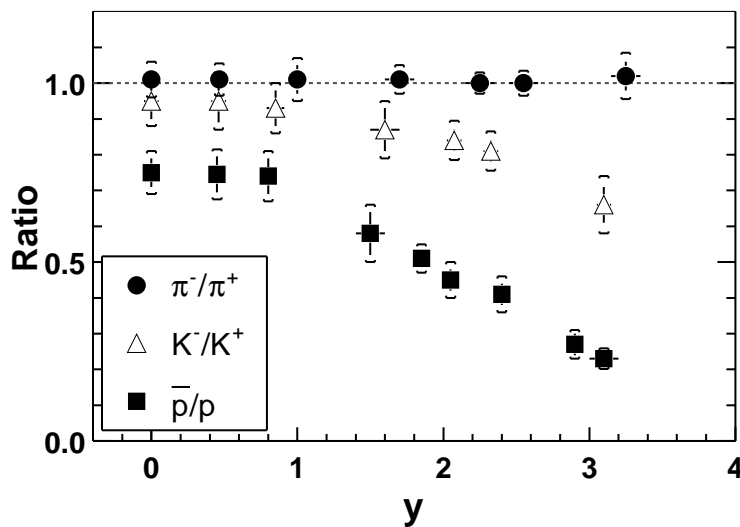


Figure 5. Ratios of antiparticles to particles (pions, kaons and protons) as a function of rapidity for $\sqrt{s_{NN}} = 200$ GeV Au+Au collisions measured by the BRAHMS experiment [8].

Integration of the charged particle pseudorapidity distributions corresponding to central collisions tells us that about 4600 charged particles are produced in each of the 5% most central collisions. Since we only measure charged particles, which are predominantly pions and kaons, as may be seen from fig. 4, and not the neutrals, we multiply this multiplicity by 3/2 to obtain the total particle multiplicity of about 7000 particles.

From the measured spectra of pions, kaons and protons and their antiparticles as a function of transverse momentum we can determine the average transverse momentum for each particle species (fig. 7). This allows us to estimate the initial energy density from

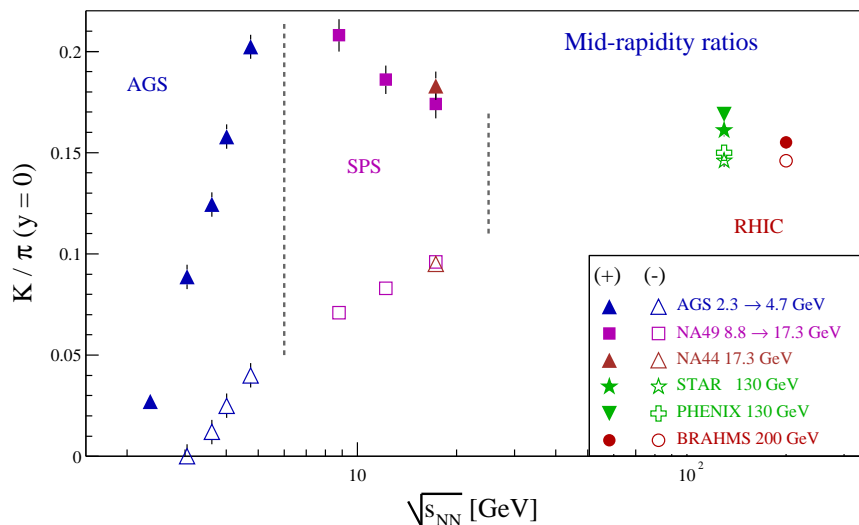


Figure 6. Ratios of kaons and pions of both charge signs as a function of center of mass energy in the nucleon-nucleon system at midrapidity. At top RHIC energy the two ratios are about the same and equal to 0.15. Preliminary BRAHMS data.

Bjorkens formula:

$$\epsilon = \frac{1}{\pi R^2 \tau} \frac{d \langle E_t \rangle}{d\eta} \quad (3)$$

where we can make the substitution $d \langle E_t \rangle = \langle m_t \rangle dN$ and use quantities from the measured spectral distributions. Since we wish to calculate the energy density in the very early stages of the collision process we may use for R the radius of the overlap disk between the colliding nuclei, thus neglecting transverse expansion. The formation time is more tricky. It is often assumed to be of the order of 1 fm/c, but it might be shorter for heavier or more energetic particles, as the uncertainty relation would tell us. Under these assumptions we find that $\epsilon > 5 \text{ GeV}/\text{fm}^3$. This value of the initial energy exceeds by a factor of 30 the energy density of a nucleus, by a factor of 10 the energy density of a baryon and by a factor of 5 the critical energy density for QGP formation that is predicted by lattice QCD calculations.

4. Is there thermodynamical and chemical equilibrium at RHIC?

The particle yields measured by BRAHMS also lend themselves to an analysis of the charged particle production in terms of the statistical model [8],[9,10,11,12]. Figure 8 shows the ratios of negative kaons to positive kaons as a function of the corresponding ratios of antiprotons to protons for various rapidities at RHIC. The data are for central collisions, and the figure also displays similar ratios for heavy ion collisions at AGS and SPS energies. There is a striking correlation between the RHIC/BRAHMS kaon and proton ratios over 3 units of rapidity. Assuming that we can use statistical arguments based on chemical and thermal equilibrium at the quark level, the ratios can be written

$$\frac{\rho(\bar{p})}{\rho(p)} = \exp\left(\frac{-6\mu_{u,d}}{T}\right) \quad (4)$$

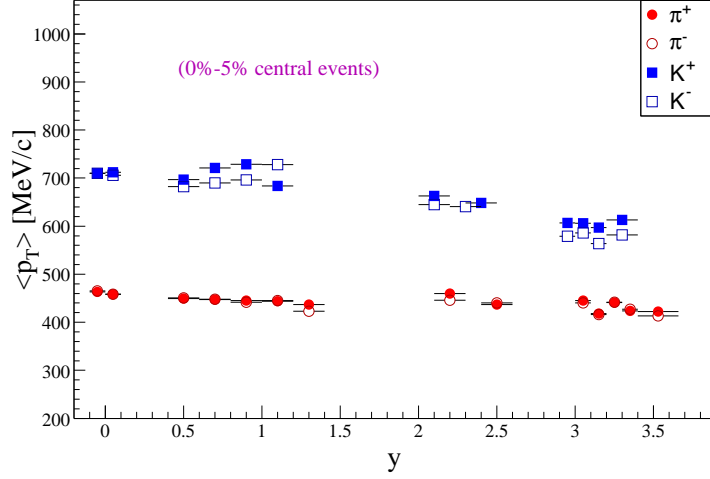


Figure 7. Distribution of average transverse momenta of pions and kaons as a function of rapidity as measured by BRAHMS. Preliminary.

and

$$\frac{\rho(K^-)}{\rho(K^+)} = \exp\left(\frac{-2(\mu_{u,d} - \mu_s)}{T}\right) = \exp\left(\frac{2\mu_s}{T}\right) \times \left[\frac{\rho(\bar{p})}{\rho(p)}\right]^{\frac{1}{3}} \quad (5)$$

where ρ , μ and T denote number density, chemical potential and temperature, respectively. From equation 4 we find the chemical potential for u and d quarks (often called the baryochemical potential) to be around 25 MeV, the lowest value yet seen in nucleus-nucleus collisions. Equation 5 tells us that for a vanishing strange quark chemical potential we would expect a power law relation between the two ratios with exponent 1/3. The observed correlation is well described by the relationship $\rho(K^-)/\rho(K^+) = \rho(\bar{p})/\rho(p)^{0.24}$, i.e. with an exponent that is close to 1/4 suggesting, a finite value of the strange quark chemical potential. A more elaborate analysis for a grand canonical ensemble assuming charge, baryon and strangeness conservation can be carried out by fitting these and many other particle ratios observed at RHIC in order to obtain the chemical potentials and temperatures. An example of such a procedure is shown in fig. 8 and displayed with the full line [13]. Here the temperature is 170MeV. The point to be made here is that the calculation agrees with the data over a wide energy range (from SPS to RHIC) and over a wide range of rapidity at RHIC. This may be an indication that the system is in chemical equilibrium over the considered \sqrt{s} and y ranges (or at least locally in the various y bins). Separate measurements at RHIC of, for example, elliptical flow also point to local equilibration around midrapidity.

5. High pt suppression. The smoking gun of QGP?

The discussion in the previous sections indicates that the conditions for particle production in a interval $|y| < 1.5-2$ are radically different than in reactions at lower energies. At RHIC the central zone is nearly baryon free, the considered rapidity interval appears to approximately exhibit the anticipated boost invariant properties, the particle production is large and dominated by pair production and the energy density appears to exceed

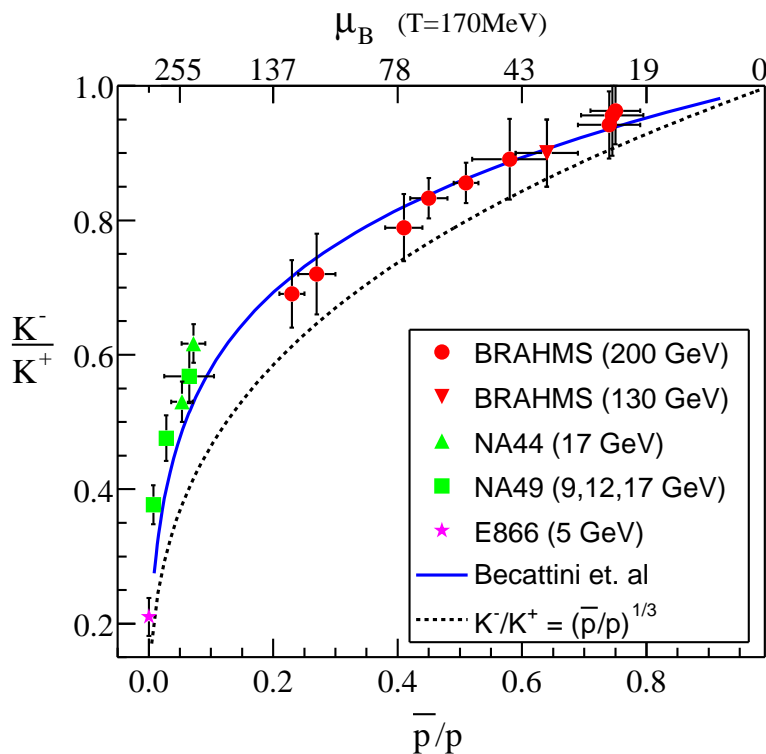


Figure 8. Correlation between the ratio of charged kaons and the ratio of antiprotons to protons. The dashed curve corresponds to equation 3 in the text. The full drawn curve is a statistical model calculation with a chemical freeze-out temperature of 177MeV.

significantly the one required for QGP formation. The overall scenario is therefore consistent with particle production from the color field, formation of a QGP and subsequent hadronization. But is this interpretation unique and can more mundane explanations based on a purely hadronic scenario be excluded? In spite of the difficulties in reconciling the high initial energy density with hadronic volumes, a comprehensive answer to this question requires the observation of an effect that is directly dependent on the partonic or hadronic nature of the formed high density zone.

Such an effect has recently been discovered at RHIC and is related to the suppression of the high transverse momentum component of hadron spectra in central Au+Au collisions as compared to scaled momentum spectra from p+p collisions [16,17,18,19]. The effect, originally proposed by Bjorken, Gyulassy and others [5,26,25] is based on the expectation of a large energy loss of high momentum partons scattered in the initial stages of the collisions in a medium with a high density of free color charges. According to QCD colored objects may lose energy by radiating gluons by bremsstrahlung. Due to the color charge of the gluons, the energy loss is proportional to the square of the depth of color medium traversed. Such a mechanism would strongly degrade the energy of leading partons resulting in a reduced transverse momentum of leading particles in the jets that emerge after fragmentation into hadrons. The STAR experiment has shown that the topology of high p_t hadron emission is consistent with jet emission, so that we may really speak about jet-suppression.

The two upper rows of fig. 9 show our [15,16] measurements of the so-called nuclear

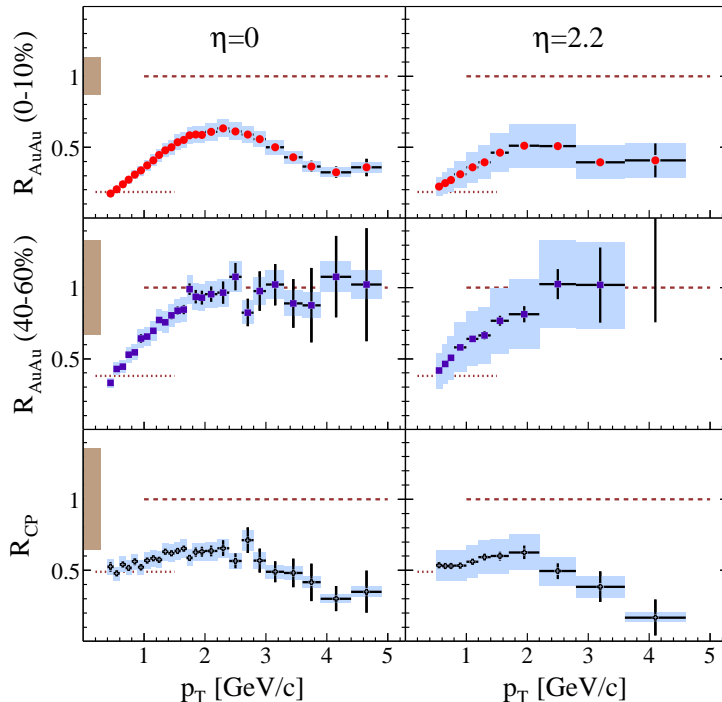


Figure 9. Nuclear modification factors R_{AuAu} as defined in the text, for central and semi-peripheral Au+Au collisions at midrapidity (left) and forward rapidity (right). The lower row shows the factor R_{CP} , i.e the ratio of the R_{AuAu} for central and peripheral collisions, which has the property of being independent of the p+p reference spectrum.

modification factors for *unidentified* charged hadrons from Au+Au collisions at rapidities $\eta = 0$ and 2.2 (this is the ph.d. work of Claus E. Jørgensen, see also his contribution at this conference). The nuclear modification factor is defined as:

$$R_{AA} = \frac{d^2 N^{AA}/dp_t d\eta}{N_{bin} d^2 N^{NN}/dp_t d\eta} \quad (6)$$

It involves a scaling of measured nucleon-nucleon transverse momentum distributions by the number of expected incoherent binary collisions, N_{bin} (see [20,21]). In the absence of any modification resulting from the 'embedding' of elementary collisions in a nuclear collision we expect $R_{AA} = 1$ at high p_t . At low p_t , where the particle production follows a scaling with the number of participants, the above definition of R_{AA} leads to $R_{AA} < 1$ for $p_t < 2 GeV/c$. In fact, it is found that $R_{AA} > 1$ for $p_t > 2 GeV/c$ in nuclear reactions at lower energy. This effect, called the Cronin effect, is associated with initial multiple scattering of high momentum partons.

Figure 9 demonstrates that, surprisingly, $R_{AA} < 1$ also at high p_t for central collisions at both pseudorapidities, while $R_{AA} \approx 1$ for more peripheral collisions. It is remarkable that the suppression that is observed at $p_t \approx 4 GeV/c$ is very large, amounting to a factor of 3 for central Au+Au collisions as compared to $p + p$ and a factor of more than 4 as

compared to the more peripheral collisions. Such large suppression factors are observed at both pseudorapidities.

It has been conjectured that the observed high p_t suppression might be the result of an entrance channel effect, for example due to a limitation in the phase space available for parton collisions related to saturation effects [27] in the gluon distributions inside the swiftly moving colliding nucleons (which have $\gamma = 100$). As a test of these ideas we have very recently determined the nuclear modification factor for 100 AGeV d + 100 AGeV Au minimum bias collisions. The resulting R_{dAu} is shown in fig. 10 where it is also compared to the R_{AuAu} for central collisions previously shown in fig. 9. No high- p_t jet suppression is observed for d+Au. In fact, the R_{dAu} distribution measured for d+Au shows the Cronin type enhancement [28] observed at lower energies [22,23,24]. At $p_t \approx 4\text{GeV}/c$ we find a ratio $R_{dAu}/R_{AuAu} \approx 5$. These observations are consistent with the smaller transverse dimensions of the overlap disk between the d and the Au nuclei and also appear to rule out strong entrance channel effects.

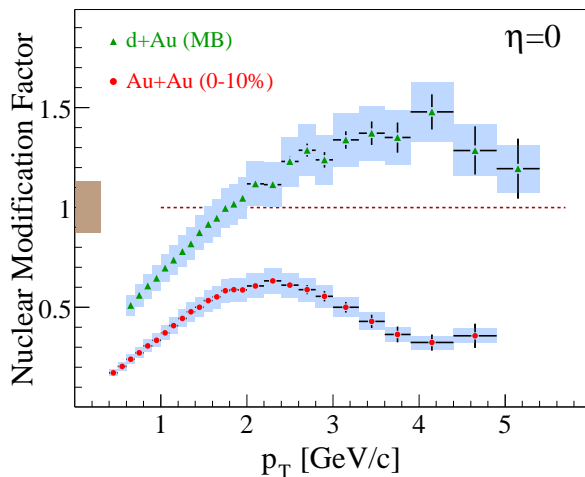


Figure 10. Nuclear modification factors measured for central Au+Au collisions and minimum bias d+Au collisions at $\sqrt{s_{NN}} = 200$ GeV, evidencing the important high p_t suppression observed in central Au+Au collisions.

The very large suppression observed in central Au+Au collisions must be quantitatively understood and will require systematic dynamic modelling. At $\eta = 0$ the particles are emitted at 90 degrees relative to the beam direction, while at $\eta = 2.2$ the angle is only about 12 degrees. In a naive geometrical picture of an absorbing medium with cylindrical symmetry around the beam direction, the large suppression seen at forward angles indicates that the suppressing medium is extended also in the longitudinal direction. Since the observed high p_t suppression is similar or even larger at forward rapidity as compared to midrapidity (see fig. 11) one might be tempted to infer a longitudinal extend of the dense medium which is approximately similar to its transverse dimensions ($R \approx 5\text{fm}$), and from this a life time longer than $5\text{fm}/c$. However, the problem is more complicated, due to the significant transverse and in particular longitudinal expansion that occurs as the leading parton propagates through the medium, effectively reducing the densities of

color charges seen. There is little doubt that systematic studies of the high p_t -jet energy loss as a function of the thickness of the absorbing medium obtained by varying the angle of observation of high p_t jets relative to the beam direction will be required in order to understand the properties of the dense medium. The BRAHMS experiment is uniquely suited among the RHIC experiments to carry out such a *QGP tomography*!

6. Conclusions and perspectives

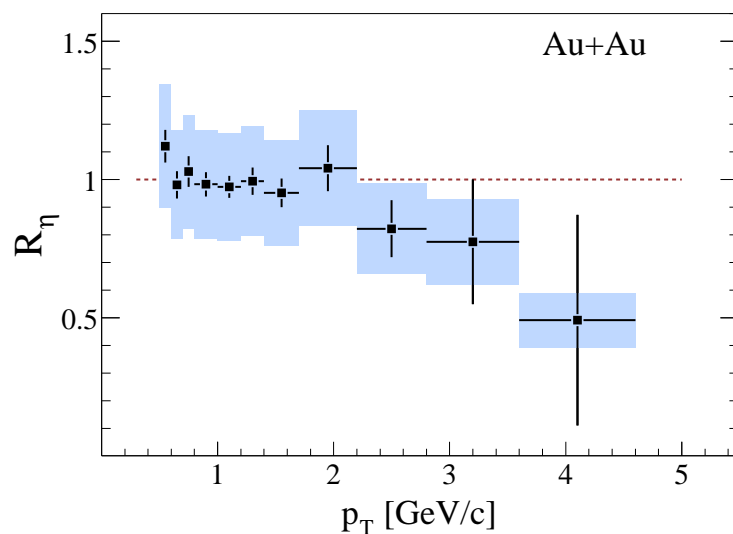


Figure 11. Ratio, R_η , of the suppression factors R_{cp} at pseudorapidities $\eta = 0$ and $\eta = 2.2$ shown in figure 9. The figure suggest that high p_t suppression persists (and is even more important) at forward rapidity than at $\eta = 0$.

The first round of RHIC experiments has clearly shown that we have moved in high energy nucleus-nucleus collisions into a qualitatively new physics domain characterized by a high degree of reaction transparency leading to the formation of a near baryon free central region. There is, nevertheless, appreciable energy loss of the colliding nuclei, so the conditions for the formation of a very high energy density zone in an interval of about $|dN/dy| < 2 \pm 0.5$ around midrapidity are present. The observation of a very large suppression of high momentum particles (jets) originating from hard scatterings in the very early stages of the collision is consistent with a significant energy loss of high momentum partons moving in a dense medium of unscreened color charges, which may be the quark gluon plasma. The next round of experiments at RHIC will afford us the opportunity to go deeper in determining the properties of the new high density state of matter that is formed, and disentangling its partonic and hadronic components [29,30]. In particular it is important to determine and understand the flavor dependence of high p_t suppression by measuring identified high p_t mesons, and likewise to compare the suppression of baryonic and mesonic jets. A systematic scan of the jet suppression as a function of the length of dense matter traversed can be carried out in both the transverse and longitudinal directions by varying the system size and the angle of observation (rapidity). Likewise, a

central future program item must be to determine, through a measurement of an excitation function, the onset of the jet suppression, which is conspicuously absent at SPS but strongly present at RHIC.

7. Acknowledgements

This work was supported by the Danish Natural Science Research Council, the division of Nuclear Physics of the Office of Science of the U.S. DOE, the Research Council of Norway, the Polish State Committee for Scientific Research and the Romanian Ministry of Research.

REFERENCES

1. M. Adamczyk *et al.*, BRAHMS Collaboration, Nucl. Instr. and Meth., **A499** (2003) 437.
2. I. G. Bearden *et al.*, BRAHMS Collaboration, Phys. Lett. **B523**, 227 (2001) and Phys. Rev. Lett. **88**, 202301 (2002).
3. BRAHMS collaboration Nucl. Phys. **A715**, 171c (2003) and *ibid* p. 482c, and P. Christiansen, Ph. D. thesis, Univ. Copenhagen, June 2003.
4. Phys. Rev. **C52**, 26(1995).
5. J. D. Bjorken, Phys. Rev. **D27**, 140 (1983).
6. C. Adler *et al.*, STAR Collaboration, Phys. Rev. Lett. **89**, 092301 (2002) and K. Adcox *et al.*, PHENIX collaboration, *ibid* p. 092302.
7. B. B. Back *et al.*, PHOBOS Collaboration, Phys. Rev. Lett. **88**, 022302 (2002).
8. I. G. Bearden *et al.*, BRAHMS Collaboration, Phys. Rev. Lett. **90**, 102301 (2003) and Phys. Rev. Lett. **90**, 112305 (2003) and refs. therein.
9. P. Koch *et al.*, Phys. Rep. **142** (1986) 167.
10. J. Cleymans *et al.* Z. Phys. **C57** (1993) 135.
11. J. Cleymans *et al.* Nucl. Phys. **A566** (1994) 391.
12. P. Braun-Munzinger *et al.*, Phys. Lett. B **518**, 41 (2001).
13. F. Becattini *et al.*, Phys. Rev. **C64**, 024901 (2001) and private communication.
14. D. Ouerdane, Ph.D. thesis, Univ. Copenhagen, August 2003.
15. BRAHMS collaboration Nucl. Phys. **A715** 741c (2003).
16. A. Arsene *et al.* Phys. Rev. Lett **91**, 072305 (2003).
17. C. Adler *et al.* Phys. Rev. Lett. **89**, 202301(2002) and Phys. Rev. Lett **91**, 072304 (2003).
18. K. Adcox *et al.* Phys. Rev. Lett. **88**, 022031(2002) and S. S. Adler *et al.* Phys. Rev. Lett **91**, 072302 (2003).
19. B. B. Back *et al.* nucl-ex/0302015 and Phys. Rev. Lett **91**, 072302 (2003).
20. C. Albajar *et al.* Nucl. Phys. **B355** 261 (1990).
21. J. Adams *et al.*, nucl-ex/0305015.
22. M. M. Aggarwal *et al.*, Eur. Phys. J. **C18** 651 (2001).
23. H. Appelshäuser *et al.*, Phys. Rev. Lett. **82** 2471 (1999).
24. G. Agakishiev *et al.*, hep-ex/0003012.
25. X. N. Wang and M. Gyulassy, Phys. Rev. Lett. **68**, 1480(1992).
26. M. Gyulassy and M. Plümer, Phys. Lett. **B243**, 432 (1990).

27. D. Kharzeev, E. Levin, L. McLerran, Phys. Lett. **B561** (2003) 93.
28. J. W. Cronin *et al.*, Phys. Rev. **D11** 3105 (1975).
29. I. Vitev, Phys. Lett. **B562**, 36 (2003) and M. Gyulassy *et al.* nucl-th/0302077.
30. K. Gallmeister, C. Greiner, Z. Xu, Phys. Rev. **C67** (2003) 044905.